

## EFFECT OF THE CORIOLIS FORCE ON CONVECTION IN A DEEP LAKE: NUMERICAL EXPERIMENT

E. A. Tsvetova

UDC 551.481.1+519.6

*Convection in a deep lake at temperatures close to the temperature of maximum density (TMD) is studied on the basis of a quasi-two-dimensional nonhydrostatic model of hydrothermodynamics with allowance for the compressibility of water. The rotation of the Earth is accounted for in the model by two components of the Coriolis force. Convection in deep lakes is influenced by the fact that the TMD is found to be dependent on pressure and salinity. Results are compared from three numerical experiments: without allowance for the Coriolis force, and with one and two Coriolis parameters. The results demonstrate the substantial effect of the Coriolis force, which shows the need to account for it in modeling convective processes in natural objects.*

**Introduction.** The debate over the need to account for the rotation of the Earth in the modeling of hydrodynamic processes that take place in the atmosphere, the ocean, and large bodies of water has long been put an end. In problems of geophysical hydrodynamics, this issue is resolved unambiguously in favor of having to account for the force. The validity of this conclusion is supported by the fact that the geostrophic balance, i.e., the balance between the pressure gradient and the Coriolis force, is almost exactly maintained for all three types of motion that occur in natural objects. However, in accordance with tradition, in almost all numerical models the Coriolis force is represented only by the single parameter  $l \equiv 2\Omega \sin\varphi$ , where  $\Omega$  is the rotational velocity of the Earth and  $\varphi$  is the latitude. As regards the second parameter,  $k \equiv 2\Omega \cos\varphi$ , its effect is assumed to be small, and it is ignored. Omitting the second component of the Coriolis force is sometimes valid. In fact, in the modeling of large-scale natural processes, a difference of three orders of magnitude between the horizontal and vertical dimensions of the regions to be studied gives the same difference in the characteristic scales of the horizontal and vertical components of the velocity vector. Thus, if the object of the investigation is other than to model convection, discarding the second component can appreciably simplify the formulation of the problem and make it possible to replace the complete equation for vertical velocity by its approximate analog, namely, the hydrostatic equation. Obvious complications arise in traditional formulations of problems with the single parameter  $l$  when it is necessary to examine equatorial regions or nearby regions, in which  $l$  is equal to or close to zero. However, this extreme case is not of interest to us here. Situations in which there is no special reason to give preference to one component over the other even arise at the middle latitudes, where the vertical and horizontal characteristic scales of motion are comparable. One of the most interesting examples of processes of this type that are observed in nature is convection in the cold fresh water of lake Baikal.

The goal of this investigation is to analyze the effect of parameters that account for the Earth's rotation on hydrothermal processes in bodies of water. The study is performed within the framework of a numerical model that we use to examine the convective mixing in a deep lake.

**Mathematical Model.** The system of equations being used expresses the laws of conservation of momentum, mass, and energy for a compressible fluid. It is assumed that all of the characteristics of the processes are uniform along the north-directed  $y$  coordinate and that motion occurs in the  $x$ - $z$  plane. The

---

Computer Center, Siberian Division, Russian Academy of Sciences, Novosibirsk 630090. Translated from *Prikladnaya Mekhanika i Tekhnicheskaya Fizika*, No. 4, pp. 127–134, July–August, 1998. Original article submitted January 27, 1997.

$x$  axis is directed to the east and the  $z$  axis is directed downward. The system includes three equations of motion for the components of the velocity vector  $u$ ,  $v$ , and  $w$  in the directions  $x$ ,  $y$ , and  $z$ , respectively,

$$\frac{du}{dt} - lv - kw = -\frac{1}{\rho} \frac{\partial p'}{\partial x} + \frac{\partial}{\partial z} \nu \frac{\partial u}{\partial z} + \frac{\partial}{\partial x} A \frac{\partial u}{\partial x}; \quad (1)$$

$$\frac{dv}{dt} + lu = \frac{\partial}{\partial z} \nu \frac{\partial v}{\partial z} + \frac{\partial}{\partial x} A \frac{\partial v}{\partial x}; \quad (2)$$

$$\frac{dw}{dt} + ku = -\frac{1}{\rho} \frac{\partial p'}{\partial z} + g \frac{\rho'}{\rho} + \frac{\partial}{\partial z} \nu \frac{\partial w}{\partial z} + \frac{\partial}{\partial x} A \frac{\partial w}{\partial x}. \quad (3)$$

The continuity equation for a compressible fluid has the form

$$\frac{\partial \rho}{\partial t} + \frac{\partial \rho u}{\partial x} + \frac{\partial \rho w}{\partial z} = 0. \quad (4)$$

The redistribution of heat in the body of water is described by the equation

$$\frac{dT}{dt} - \Gamma \frac{dp}{dt} = \frac{\partial}{\partial z} \nu_T \frac{\partial T}{\partial z} + \frac{\partial}{\partial x} \mu \frac{\partial T}{\partial x}. \quad (5)$$

We augment the system by the nonlinear equation of state

$$\rho = \rho(p, T, S_0). \quad (6)$$

Here  $l$  and  $k$  are the Coriolis parameters, which are almost always regarded as constant due to the relatively small horizontal dimensions of lakes;  $p$  is the pressure and  $p'$  is the deviation of the local pressure from the local hydrostatic value  $p_h$  when the system is at the specified values of temperature  $T^0(z)$  and salinity  $S_0$ ,  $p'(x, z, t) = p(x, z, t) - p_h(z)$ ;  $\rho$  is the density and  $\rho'$  is the corresponding deviation of density,  $\rho'(x, z, t) = \rho(x, z, t) - \rho_h(z)$ ;  $A$ ,  $\nu$ ,  $\mu$ , and  $\nu_T$  are the coefficients of eddy diffusion,  $T$  is the temperature,  $\Gamma$  is the adiabatic gradient,  $\Gamma = \alpha T_a / (\rho c_p)$ ,  $T_a$  is the absolute temperature,  $c_p$  is the isobaric specific heat,  $S_0$  is salinity, and  $\alpha$  is the coefficient of thermal expansion.

System (1)–(6) will be examined in the region  $D_t = D \times [0, t_k]$ , where  $D$  is the range of variation of the space variables  $(x, z)$  and  $[0, t_k]$  is the time interval. The relief of the bottom is assumed to be a smooth function of the horizontal coordinate. The boundary and initial conditions are as follows:

$$\nu \frac{\partial u}{\partial z} = -\frac{\tau_x}{\rho}, \quad \nu \frac{\partial v}{\partial z} = -\frac{\tau_y}{\rho}, \quad \nu_T \frac{\partial T}{\partial z} = -\frac{Q}{\rho c_p}; \quad (7)$$

$$p = p_a, \quad w = -\frac{1}{g\rho} \frac{\partial p'}{\partial t} \quad (8)$$

on the surface for  $z = 0$ ,

$$u = v = w = 0, \quad \frac{\partial T}{\partial N} = 0 \quad (9)$$

on the bottom for  $z = H(x)$ , and

$$u = v = w = 0, \quad \frac{\partial T}{\partial N} = 0 \quad (10)$$

on the lateral boundaries;

$$\varphi = \varphi^0(x, z), \quad \varphi = (u, v, w, T, p, \rho). \quad (11)$$

are the initial conditions for  $t = 0$ . Here  $\partial/\partial N$  is a derivative with respect to the conormal:

$$\frac{\partial}{\partial N} = \mu \cos(\mathbf{n}, x) \frac{\partial}{\partial x} + \nu_T \cos(\mathbf{n}, z) \frac{\partial}{\partial z}, \quad (12)$$

where  $\mathbf{n}$  is the vector of the outer normal to the boundary of the region,  $p_a$  is the atmospheric pressure,  $\tau_x$ , and  $\tau_y$  represent the wind stress,  $Q$  is the heat flow on the surface, and  $\varphi^0(x, z)$  are assigned functions.

The equation of state (6), used in the model, is especially suited for limnologic purposes [2], i.e., the ranges of  $T$ ,  $p$ , and  $S$  correspond to the values encountered in lakes. In accordance with this, the equation of density is a nonlinear function of temperature, pressure, and salinity. In the version of the model used here, salinity is assigned a constant value of 0.098 g/kg. The adiabatic temperature gradient, the coefficient of thermal expansion, the specific heat, and other thermodynamic quantities needed in the model are also calculated from formulas given in [2].

One of the most important problems in modeling convection is turbulence parameterization. Motions that occur on the subnetwork scale and are not reproduced directly in the model are parameterized by means of second-order diffusion operators. As is customary in oceanology, different methods are used to describe horizontal and vertical processes. In the numerical experiments described in this paper, the horizontal turbulence coefficients were assumed to be constant, while functional dependences on the gradient Richardson number were used for the vertical coefficients.

The numerical algorithm is based on the method of branching in relation to physical processes [3]. The variational principle [4] is used to construct approximations (1)–(12), which are balanced with respect to energy. In accordance with the concept of branching, the problem is solved in several stages at each time step. The approach that we apply in the solution of the problem is described in more detail in [5].

We used the above-described model and some modifications of it to perform a series of studies involving the modeling of Coriolis processes in a deep lake [1, 6, 7]. Of particular interest are the experiments in which the thermal bar is studied. Thermal bars develop in dimictic lakes twice a year, in spring and fall. This phenomenon is especially important in lake Baikal, since it plays a key role in renewing the deep waters of the lake [8–13]. It was hypothesized in [8–13] that intensive water exchange occur at the front of a thermal bar and that the decisive factor in this exchange is the decrease in the TMD with increase in pressure.

In contrast to our formulation of the problem, in [14] the thermal bar in deep lakes was described by two two-dimensional models, namely, a hydrostatic model and a nonhydrostatic model. The Coriolis force was not considered in either model, and the dependence of density on pressure was absent in the equations of state. In our opinion, such omissions make it impossible to achieve a high degree of accuracy in evaluating the temperature distribution and, thus, any of the other components of the state function. Nevertheless, the authors of [14] assert that such models can describe the basic features of the renewal of deep waters near the sides of a deep lake.

Our goal is to analyze differences in the results of calculations performed using models with one and two Coriolis parameters. Since the thermal bar also figure into our calculations, it is natural to additionally examine the case where rotation is not considered. Such a situation corresponds in part to the conditions of the experiments in [14]. In the present case, the results obtained from the modeling can be regarded as an estimate of the effect of the parameters of the problem on the characteristics of the thermal bar and, thus, on processes involved in the renewal of deep waters in a lake.

**Numerical Experiments.** The numerical experiments are performed using a single formulation of the problem. The changes that distinguish one experiment from another are not taken into account in the algorithm. They are accounted for by assigning suitable values to the parameters that pertain solely to the Coriolis force. We compare the results of three numerical experiments:

- No. 0.  $l = 0$  and  $k = 0$ ;
- No. 1.  $l \neq 0$  and  $k = 0$ ;
- No. 2.  $l \neq 0$  and  $k \neq 0$ .

The two-dimensional region in which the problem is solved is a trapezoidal cavity. The horizontal dimension along the upper boundary is 40 km. Short vertical walls bound the region on the left and right. The angles of inclination of the sides of the trapezoid are identical. The maximum depth is 960 m. The region is covered by a regular grid with cells having the dimensions  $\Delta x = 80$  m and  $\Delta z = 20$  m, i.e., the calculations are performed on a grid with  $501 \times 49$  points. The time step is  $\Delta t = 60$  sec. The coastal slopes of the lake are approximated by line segments that are parallel to the coordinate axes. We are examining the problem of the vernal heating of a deep lake. The parameters of the model are chosen so that they are within the

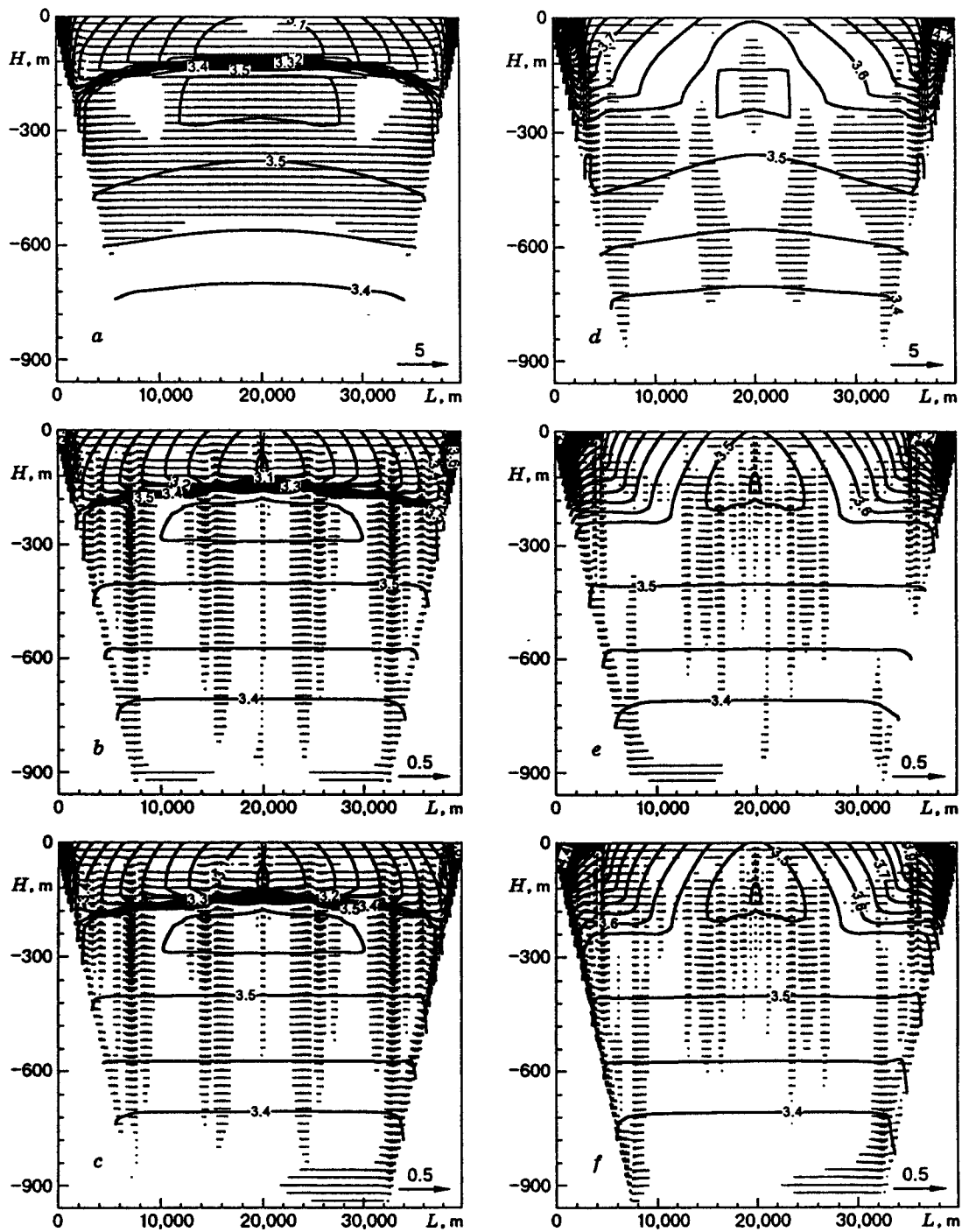


Fig. 1. Flow field and temperature isolines: experiment Nos. 0, 1, and 2 in ten (a, b, and c) and twenty (d, e, and f) days after the beginning of the experiment.

ranges of variation corresponding to conditions at lake Baikal. The initial temperature field is assumed to be uniform in the horizontal direction and variable in the vertical direction. The vertical profile, based on measurements made on the Listvenichnoe–Tankhoi section of the lake on 06.01.77, schematically represents a typical vernal temperature profile in lake Baikal. The maximum temperature is 3.6°C at a depth of 250 m, in the region of the so-called mesothermal maximum. The profile includes a clearly visible thermocline at the depths 100–150 m. The temperature at the surface is 2.61°C. Agreement is obtained between the initial distribution of temperature  $T^0$ , pressure  $p_h$ , and density  $\rho_h$  by solving a system of two equations with two unknowns. One of these equations is the equation of state (6), while the second equation is the hydrostatic equation  $\partial p_h / \partial z = g\rho_h$ . The latter equation is solved with the boundary condition from (9). The system is solved by the fourth-order Runge–Kutta method.

At the initial moment (the state of rest), the components of the velocity vector and the deviations of pressure and density from their hydrostatic values are all equal to zero. The wind stress on the surface is assumed to be zero for the duration of the experiment. Besides being interesting from a methodological viewpoint, the use of this approximation is justified by the fact that observations have shown that the wind is almost always weak and variable at lake Baikal during the spring. The natural source of motion is the flux of heat on the surface, which is given as a function of the horizontal coordinate  $Q(x) = c - d \sin(\pi x/L)$ . Here  $c = 167.3 \text{ J}/(\text{m}^2 \cdot \text{sec})$ , which corresponds to the average data for June. The following values were chosen for the other parameters:  $d = 0.002$  and  $A = \mu = 0.1 \text{ m}^2/\text{sec}$ .

The results of the numerical modeling are shown in Fig. 1, where the flow fields are combined with the temperature fields. The isotherms are drawn every 0.05°C. Only each fourth point of the grid in the horizontal direction is represented in the vector fields. Figure 1a and d shows the results of experiment No. 0, Fig. 1b and e shows the results of experiment No. 1, and Fig. 1c and f shows the results of experiment No. 2. Of fundamental importance in each experiment is the nonlinear behavior of density in relation to temperature and pressure.

Figure 1a–c pertains to the moment of time  $t = 10$  days from the beginning of the experiments. These parts of Fig. 1 have several features in common. It is apparent that the surface temperature near the shore approaches the TMD, the isolines are tightly bunched, and they are nearly vertical, i.e., intensive mixing occurs in the depth direction from the surface to the slope. Two circulation cells, located near the shore, can be seen in all parts of Fig. 1. These cells are formed by a thermocline, which “chokes” the flows descending along the slope and prevents them from initially continuing downward along the slope.

While the flow patterns and temperature fields in Fig. 1a and c were calculated with allowance for the Coriolis force and differ from one another only in certain details, Fig. 1a shows a completely different flow pattern and a different behavior of the isolines of the temperature field. The flow velocity in experiment No. 0 is significantly greater than the flow velocity in the other two experiments. This can be seen from a comparison of the corresponding parts of the figure (the scale of the vectors in Fig. 1a is different from the scale chosen for Figs. 1b and c). The flow pattern seen without allowance for rotation (Fig. 1a) is of a “global” character: descent along the slopes and ascent in the center. The pattern is completely symmetrical relative to the central vertical axis of the region. It is apparent from Fig. 1b and c that allowance for rotation makes the scales of motion finer, the flow fields in this case exhibiting a complex cellular structure which changes over time.

The amount of heat reaching the surface was the same in all of the experiments, but it was redistributed differently in the thickness direction. This difference is shown by the position of the isotherms. For example, in experiment No. 0 (Fig. 1a) the horizontal temperature gradients are smaller at the epilimnion and the thermocline are positioned higher than in the other variants. A comparison of experiment Nos. 1 and 2 (Fig. 1b and c) shows significant differences in the behavior of the isotherms and the flow vectors only near the shore.

Figure 1d–f shows data for 20 days after the beginning of the experiment. Intensive mixing completely eliminates the thermocline that had been located at a depth of 100–150 m in the initial temperature field before descending to a depth of about 200 m over 10 days. A new thermocline begins to be formed near the surface. As regards the behavior of the isotherms at the 300-m level, it is seen that the isolines in that

part of the region are nearly horizontal in all of the experiments before sharply changing direction. The line that connects the points of the maximum gradients on the isotherms is the front line. It coincides with the locus where the temperature in situ is equal to the local TMD,  $T = T_*(p(x, z, t), S_0)$ , i.e., by definition, a thermocline must pass near this line. Two thermal bars (one on the left and one on the right) are visible in all the parts of Fig. 1. These thermal bars move a substantial distance from the shores, where they began to form. Thus, thermal bars were obtained in all the experiments. We shall see how the results of the calculations differ.

As at the previous moment of time, all of the differences noted above are still in existence. Experiment Nos. 1 and 2 (Fig. 1e and f) show similar results, while the experiment without rotation (Fig. 1d) differs from them in the structure of the temperature and flow fields. An analysis of the calculated results leads to the conclusion that the Coriolis force distorts the process and has the same effect as stratification. The same conclusion was reached by the authors of the theoretical study [15], which examined the properties of the solution of a hydrodynamic problem describing a stratified rotating liquid.

Finally, a comparison of the results in Fig. 1e and f convincingly shows that, as at the previous moment of time, there are significant differences in the behavior of the hydrodynamic characteristics near the shore in the experiments in which allowance is made for one and two components of the Coriolis force.

From the viewpoint of the geophysical significance of the results, the studies that we have performed with the use of numerical modeling show that water exchange between surface waters and deep waters may actually occur as a result of the flows which accompany the thermal bar. Such flows usually reach the underwater slopes. These findings are consistent with the above-mentioned hypothesis [8–13]. It also follows from an analysis of the situation as a whole that the water exchange occurs not just near the thermal bar. It takes place throughout the region, due to convection that involves alternating descending and ascending motions and reaches the maximum depths. The horizontal and vertical dimensions of the convection cells determined in the calculations are comparable to one another, and the character of the water exchange is determined by the dynamics of the thermocline and the regions in which the local water temperature coincides with the TMD for the local conditions.

**Conclusion.** Numerical experiments performed on the basis of the above-described model permit the conclusion that at least the parameter  $l$  of the Coriolis force must be considered in modeling numerically convection in deep lakes. The role of the second parameter also seems important to us, especially in a metalimnion and a hypolimnion. It was discovered that a difference exists in the processes that occur near the western and eastern shores of the lake due to the second component of the Coriolis effect. To definitively explain the role of the parameter  $k$ , we shall attempt to continue our research on a three-dimensional model and, using the same formulation of the problem, also to take into account irregularities along the second horizontal coordinate. However, it has already become apparent from the series of experiments completed thus far that as long as the Earth's rotation is taken into consideration, the use of one or two Coriolis parameters in the model does not fundamentally alter the structure of the solution — in the way that ignoring the Coriolis force altogether would.

This work was supported by the Russian Foundation for Fundamental Research (Grant No. 94-05-16106).

## REFERENCES

1. E. A. Tsvetova, "Specific manifestations of convection in deep lakes," *Mat. Probl. Ekologii*, No. 2, 181–189 (1996).
2. C. T. Chen and F. J. Millero, "Precise thermodynamic properties for natural waters covering only the limnological range," *Limnol. Oceanogr.*, **31**(3); 657–662 (1986).
3. G. I. Marchuk, *Numerical Solution of Problems of the Dynamics of the Atmosphere and the Ocean* [in Russian], Gidrometeoizdat, Leningrad (1974).
4. V. V. Penenko, *Methods of Numerically Modeling Atmospheric Processes* [in Russian], Gidrometeoizdat, Leningrad (1981).

5. E. A. Tsvetova, "Compressibility effects in lake hydrodynamics," in: *Bull. of the Novosibirsk Computing Center, Ser. Numerical Modeling in Atmosphere, Ocean, and Environment Studies*, No. 1 (1993), pp. 91–103
6. E. A. Tsvetova, "A numerical model of thermal bar in lake Baikal," in: *Bull. of the Novosibirsk Computer Center, Ser. Numerical Modeling in Atmosphere, Ocean, and Environment Studies*, No. 2, (1995), pp. 85–100.
7. E. A. Tsvetova, "Convective currents associated with the thermal bar of lake Baikal," in: A. S. Alekseev and N. S. Bakhvalov (eds.), *Adv. Math.: Computations and Appl.*, NCC Publisher, Novosibirsk (1995), pp. 386–393.
8. M. N. Shimaraev and N. G. Granin, "Thermal stratification and convection mechanism in lake Baikal," *Dokl. Akad. Nauk SSSR*, **321**, No. 2, 831–835 (1991).
9. M. N. Shimaraev, M. A. Grachev, D. M. Imboden, et al., "International geophysical experiment in lake Baikal: deep-water renewal processes in the spring," *Dokl. Ross. Akad. Nauk*, **343**, No. 6, 824–827 (1995).
10. M. N. Shimaraev, V. M. Domyшева, and L. A. Gorbunova, "Dynamics of oxygen in lake Baikal during the spring mixing period," *Dokl. Ross. Akad. Nauk*, **347**, No. 6, 814–817 (1996).
11. M. N. Shimaraev and N. G. Granin, "Deep ventilation of lake Baikal waters due to spring thermal bars," *Limnol. Oceanogr.*, **38**, No. 5, 1068–1072 (1993).
12. M. N. Shimaraev, V. I. Verbolov, et al., "Physical Limnology of Lake Baikal: A Review," Print No. 2, Baikal Int. Center for Ecological Res. (1994).
13. R. F. Weiss, E. C. Carmack, and V. M. Koropalov, "Deep water renewal and biological production in lake Baikal," *Nature*, **349**, 665–669 (1991).
14. O. B. Bocharov, O. F. Vasil'ev, V. I. Kvon, and T. É. Ovchinnikova, "Mathematical modeling of a thermal bar in a deep lake," *Dokl. Ross. Akad. Nauk*, **349**, No. 4, 530–532 (1996).
15. V. N. Maslennikova and I. M. Petunin, "Asymptote for  $t \rightarrow \infty$  in the solution of an initial-boundary-value problem in the theory of internal waves," *Differ. Uravn.*, **31**, No. 5, 823–828 (1995).